Evaluation of simulated biomass damage in forest ecosystems induced by ozone against observation-based estimates

Martina Franz[1,2], Rocio Alonso[4], Almut Arneth[5], Patrick Büker[6], Susana Elvira[4], Giacomo Gerosa[7], Lisa Emberson[6], Zhaozhong Feng[8], Didier Le Thiec[9], Riccardo Marzuoli[7], Elina Oksanen[10], Johan Uddling[11], Matthew Wilkinson[12], and Sönke Zaehle[1,3]

[1]Biogeochemical Integration Department, Max Planck Institute for Biogeochemistry, Jena, Germany
[2]International Max Planck Research School (IMPRS) for Global Biogeochemical Cycles, Jena, Germany
[3]Michael Stifel Center Jena for Data-driven and Simulation Science, Jena, Germany
[4]Ecotoxicology of Air Pollution, CIEMAT - Research Center for Energy, Environment and Technology, Avda. Complutense 40, edif.70, Madrid 28040, Spain
[5]Karlsruhe Institute of Technology (KIT), Department of Atmospheric Environmental Research (IMK-IFU), Garmisch-Partenkirchen, Germany
[6]Stockholm Environment Institute at York, Environment Dept., University of York, YO10 5NG, United Kingdom
[7]Department of Mathematics and Physics, Catholic University of Brescia, via Musei 41, Brescia (Italy)
[8]State Key Laboratory of Urban and Regional Ecology, Research Center for Eco-Environmental Sciences, Chinese Academy of Sciences, Shuangqing Road 18, Haidian District, Beijing, 100085, China
[9]Inra, Université de Lorraine, AgroParisTech, Silva, F-54280 Champenoux, France
[10]Department of Environmental and Biological Sciences, University of Eastern Finland, 80101 Joensuu, Finland
[11]Department of Biological and Environmental Sciences, University of Gothenburg, Gothenburg, Sweden
[12]Centre for Sustainable Forestry and Climate Change, Forest Research, UK

Correspondence: Martina Franz (mfranz@bgc-jena.mpg.de)

Abstract.

Regional estimates of the effects of ozone pollution on forest growth depend on the availability of reliable injury functions that estimate a representative ecosystem response to ozone exposure. A number of such injury functions for forest tree species and forest functional types have recently been published and subsequently applied in terrestrial biosphere models to estimate regional or global effects of ozone on forest tree productivity and carbon storage in the living plant biomass. The resulting impacts estimated by these biosphere models show large uncertainty in the magnitude of ozone effects predicted. To understand the role that these injury functions play in determining the variability of estimated ozone impacts, we use the O-CN biosphere model to provide a standardised modelling framework. We test four published injury functions describing the leaf-level, photosynthetic response to ozone exposure (targeting the maximum carboxylation capacity of Rubisco (V_{cmax}) or net photosynthesis) in terms of their simulated whole-tree biomass responses against field data from 23 ozone filtration/fumigation experiments conducted with European tree species at sites across Europe with a range of climatic conditions. Our results show that none of these previously published injury functions lead to simulated whole-tree biomass reductions in agreement with the observed dose-response relationships derived from these field experiments, and instead lead to significant over- / or underestimations of the ozone effect. By re-parameterising these photosynthetic based injury functions we develop linear, plant

functional type specific dose-response relationships, which provide accurate simulations of the observed whole-tree biomass response across these 23 experiments.

1 Introduction

Ozone is a phytotoxic air pollutant which enters plants mainly through the leaf stomata, where reactive oxygen species (ROS) are formed that can injur essential leaf functioning (Ainsworth et al., 2012). Ozone induced declines in net photosynthesis (Morgan et al., 2003; Wittig et al., 2007) have been observed as the result of injury of the photosynthetic apparatus, increased respiration rates caused by investments in repair of injury, as well as the production of defence compounds (Wieser and Matyssek, 2007; Ainsworth et al., 2012). At the leaf-scale, ozone injury occurs and accumulates, when the instantaneous stomatal ozone uptake of leaves surpasses the ability of the leaf to detoxify ozone (Wieser and Matyssek, 2007). These effects are likely the primary cause for reduced rates of net photosynthesis and decreased supply of carbon and energy for growth and net primary production (NPP), which contributes to the commonly observed ozone-induced reductions in leaf area and plant biomass (Morgan et al., 2003; Lombardozzi et al., 2013; Wittig et al., 2009). Changes in tropospheric ozone abundance and associated changes in ozone-induced injury thus have the potential to affect the ability of the terrestrial biosphere to sequester carbon (Harmens and Mills, 2012; Oliver et al., 2017). However, a quantitative understanding of the effect of ozone pollution on forest growth and carbon sequestration at the regional scale is still lacking. Terrestrial biosphere models can be used to obtain regional or global estimates of ozone damage based on an understanding of how ozone affects plant processes leading to C assimilation and growth. Modelling algorithms to estimate regional or global impacts of ozone on gross primary production (GPP) have been developed for several of these terrestrial biosphere models (Sitch et al., 2007; Lombardozzi et al., 2012a, 2015; Franz et al., 2017; Oliver et al., 2017). However, simulated reductions in GPP due to ozone induced injury vary substantially between models and model versions (Lombardozzi et al., 2012a, 2015; Franz et al., 2017; Sitch et al., 2007).

This uncertainty is predominantly due to the different approaches that these models use to relate ozone uptake (or ozone exposure) to reductions in whole-tree biomass, and in the exact parameterisation of the injury functions and dose-response relationships applied (Karlsson et al., 2004; Pleijel et al., 2004; Wittig et al., 2007; Lombardozzi et al., 2012a, 2013). The injury functions employed by current terrestrial biosphere models differ decidedly in their slope (i.e. the change in injury per unit of time-integrated ozone uptake), intercept (ozone injury at zero time-integrated ozone uptake), and in their assumed threshold, below which the ozone uptake rate is considered sufficiently low that ozone will be detoxified before any injury occurs (Karlsson et al., 2004; Pleijel et al., 2004; Lombardozzi et al., 2012a). For example, Sitch et al. (2007) relates the instantaneous ozone uptake exceeding a flux threshold to net photosynthetic injury via an empirically derived factor. An alternative approach has been to relate ozone injury to net photosynthesis in response to the accumulated ozone uptake rather than to the instantaneous ozone uptake as in Sitch et al. (2007), e.g. by using the $CUOY$, which refers to the cumulative canopy O_3 uptake above a flux threshold of $Y\ nmol\,m^{-2}\,s^{-1}$ (Wittig et al., 2007; Lombardozzi et al., 2012a, 2013; Cailleret et al., 2018).

The effect of ozone on plant growth has been investigated by ozone filtration/fumigation experiments either at the individual experimental level or by pooling data from multiple experiments that have been conducted according to standardised

experimental method. These experiments typically rely on small trees or saplings. A challenge in developing and testing process-based models of ozone damage from these ozone fumigation experiments is that often only the difference in biomass accumulation between plants grown in an ozone treatment and in ambient or charcoal-filtered air at the end of the experiment are reported. Data from these studies provide evidence for a linear, species-specific relationship between accumulated ozone uptake and reductions in plant biomass (Pleijel et al., 2004; Mills et al., 2011; Nunn et al., 2006, e.g.). Sitch et al. (2007) for instance calibrated their instantaneous leaf-level injury function between ozone uptake and photosynthesis by relating simulated annual net primary production and accumulated ozone uptake to observed biomass dose-response relationships developed by Karlsson et al. (2004) and Pleijel et al. (2004), where biomass/yield damage is related to the Phytotoxic Ozone Dose ($PODy$). The $PODy$ refers to the accumulated ozone uptake above a flux threshold of $y\ nmol\,m^{-2}\,s^{-1}$ by the leaves representative of the upper canopy leaves of the plant. Such an approach applies biomass dose-response relationships of young trees to mature trees. However, the effects of ozone on leaf physiology (e.g. net photosynthesis and stomatal conductance) or plant carbon allocation may differ between juvenile and adult trees (Hanson et al., 1994; Samuelson and Kelly, 1996; Kolb and Matyssek, 2001; Paoletti et al., 2010). Whether or not biomass dose-response relationships can be used to calibrate injury functions for mature trees is uncertain.

An alternative approach is to directly simulate ozone injury to photosynthesis, which may have been a major cause for the observed decline in plant biomass production (Ainsworth et al., 2012). Possible injury targets in the simulations can be for example the net photosynthesis or leaf-specific photosynthetic activity (such as represented by the maximum carboxylation capacity of Rubisco, V_{cmax}). For instance Lombardozzi et al. (2012a) based their injury function on an experimental study involving a single forest tree species, whereas more recent publications (e.g. Lombardozzi et al. (2015) and Franz et al. (2017)) have used injury functions from meta-analyses of a far larger-set of filtration/fumigation studies. Meta-analyses have attempted to summarise the responses of plant performance to ozone exposure across a wider range of experiments and vegetation types (Wittig et al., 2007; Lombardozzi et al., 2013; Feng and Kobayashi, 2009; Li et al., 2017; Wittig et al., 2009) and to develop injury functions for plant groups that might provide an estimate of mean plant group responses to ozone. However, these meta-analyses suffer from a lack of consistency in the derivation of either plant injury or ozone exposure, and generally report a large amount of unexplained variance. A further complication in the meta-analyses of ozone injury (e.g. Wittig et al., 2007; Lombardozzi et al., 2013) is that they have to indirectly estimate the cumulative ozone uptake underlying the observed ozone injury based on a restricted amount of data, which causes uncertainty in the derived injury functions.

Büker et al. (2015) provides an independent data set of whole-tree biomass plant responses to ozone uptake which is independent of data sets that were used to describe injury functions by Wittig et al. (2007) and Lombardozzi et al. (2013). This data set has been collected from experiments that follow a more standardised methodology to assess dose-responses and has associated meteorological and ozone data at a high time resolution that allow more accurate estimates of modelled ozone uptake to be made. These dose-response relationships describe whole-tree biomass reductions in tree seedlings derived from standardised ozone filtration/fumigation methods for eight European tree species at ten locations across Europe (see Tab. A.2 for details Büker et al., 2015). These data thus provide an opportunity to evaluate simulations of biosphere models that use leaf level injury functions (describing the effect of ozone uptake on photosynthetic variables) to estimate C assimilation, growth and

ultimately whole tree biomass against these robust empirical dose-response relationships that relate ozone exposure directly to whole tree biomass response.

Here we test four alternative, previously published ozone injury functions that target either net photosynthesis or the leaf carboxylation capacity (V_{cmax}), which have been included in state-of-the-art terrestrial biosphere models (Lombardozzi et al., 2012a, 2015; Franz et al., 2017) against these new biomass dose-response relationships by Büker et al. (2015). We incorporate these injury functions into a single modelling framework, the O-CN model (Zaehle and Friend, 2010; Franz et al., 2017). To reduce model-data mismatch, we test the functions in simulations that mimic to the extend possible the conditions of each of the experiments in the Büker et al. (2015) data-set, in particular the young age, such that we can directly compare the simulated to the observed whole-tree biomass reductions of the empirically derived dose-response relationships. This allows us to identify the contribution of these alternative injury function formulations on the simulated whole-tree biomass response. The simulated biomass dose-response relationships are then compared to the data from the experiments to evaluate the capability of the different model versions to reproduce observed dose-response relationships. Based on these comparisons we use a similar approach to that of Sitch et al. (2007) and develop alternative parameterisations of the injury functions to improve the capability of the O-CN model to simulate the whole-tree biomass responses observed in the field experiments, with the notable exception that we explicitly simulate in-fumigation experiments and the approximate age of the trees. Finally, we explore whether or not there is a substantial difference in the biomass response to ozone of young or mature trees by using a sequence of model simulations and comparing the response both in terms of whole tree biomass as well as net primary production.

2 Methods

We use the O-CN terrestrial biosphere model (Zaehle and Friend, 2010), which is an extension of the ORCHIDEE model (Krinner et al., 2005) to simulate conditions of the ozone fumigation experiments described in Büker et al. (2015). The O-CN model, an average-individual dynamic vegetation model, simulates the terrestrial coupled carbon (C), nitrogen (N) and water cycles for up to twelve plant functional types and is driven by climate data and atmospheric composition.

O-CN simulates a multi-layer canopy with up to 20 layers with a thickness of up to 0.5 leaf area index each. Net photosynthesis is calculated according to a modified Farquhar-scheme for shaded and sun-lit leaves considering the light profiles of diffuse and direct radiation (Zaehle and Friend, 2010). Leaf nitrogen concentration and leaf area determine the photosynthetic capacity. Increases of the leaf nitrogen content increase V_{cmax} and J_{max} (nitrogen specific rates of maximum light harvesting, electron transport) and hence maximum net photosynthesis and stomatal conductance per leaf area. The leaf N content is highest at the top of the canopy and exponentially decreases with increasing canopy depth (Friend, 2001; Niinemets et al., 2015). Following this net photosynthesis, stomatal conductance and ozone uptake are generally highest in the top canopy and decrease with increasing canopy depth.

Canopy-integrated assimilated carbon enters a labile non-structural carbon pool, which can either be used to fuel maintenance respiration (a function of tissue nitrogen), storage (for seasonal leaf and fine root replacement and buffer of inter-annual variability of assimilation) or biomass growth. The labile pool responds within days to changes in GPP, the long-term reserve

has a response time of several months, depending on its use to support seasonal foliage and fine root development or sustain growth in periods of reduced photosynthesis. After accounting for reproductive production (flowers and fruits), biomass growth is partitioned into leaves, fine roots, and sapwood according to a modified pipe-model (Zaehle and Friend, 2010), accounting for the costs of biomass formation (growth respiration). In other words, changes in leaf-level productivity affect the build-up of plant pools and storage, and thereby feed back on the ability of plants to acquire C through photosynthesis, or nutrients through fine root uptake.

2.1 Ozone injury calculation in O-CN

Throughout the manuscript we refer to 'injury' for the biological response to O_3 uptake at the leaf level and to 'damage' for responses of plant production, growth and biomass at the ecosystem level following Guderian (1977). The relationship between ozone uptake and injury is called 'injury function'; the relationship between ozone uptake and damage is called 'dose-response-relationship'.

Leaf-level ozone uptake is determined by stomatal conductance and atmospheric O_3 concentrations, as described in Franz et al. (2017). To mimic the conditions of the fumigation experiments with plot-level controlled atmospheric O_3 concentrations, simulations are conducted with a model version of O-CN, in which atmospheric O_3 concentrations are directly used to calculate ozone uptake into the leaves, and the transfer and destruction of ozone between the atmosphere and the surface is ignored (ATM model version in Franz et al. (2017)). Deviating from Franz et al. (2017), stomatal conductance g_{st} here is calculated based on the Ball and Berry formulation (Ball et al., 1987) as

$$g_{st,l} = g_0 + g_1 \times \frac{A_{n,l} \times RH \times f(height_l)}{C_a} \tag{1}$$

where net photosynthesis ($A_{n,l}$) is calculated as described in Zaehle and Friend (2010) as a function of the leaf internal partial pressure of CO_2, absorbed photosynthetic photon flux density on shaded and sunlit leaves, leaf temperature, as well as the nitrogen specific rates of maximum light harvesting, electron transport (J_{max}) and carboxylation rates (V_{cmax}). RH is the atmospheric relative humidity, $f(height_l)$ the water-transport limitation with canopy height, C_a the atmospheric CO_2 concentration, g_0 is the residual conductance when A_n approaches zero, and g_1 is the stomatal-slope parameter as in Krinner et al. (2005). The index l indicates that g_{st} is calculated separately for each canopy layer.

The stomatal conductance to ozone $g_{st,l}^{O_3}$ is calculated as

$$g_{st,l}^{O_3} = \frac{g_{st,l}}{1.51} \tag{2}$$

where the factor 1.51 accounts for the different diffusivity of O_3 from water vapour (Massman, 1998).

For each canopy layer the O_3 stomatal flux ($f_{st,l}$, $nmol\,m^{-2}(leaf\,area)\,s^{-1}$) is calculated from the atmospheric O_3 concentration the plants in the field experiments were fumigated with ($\chi_{atm}^{O_3}$) and $g_{st,l}$ as

$$f_{st,l} = (\chi_{atm}^{O_3} - \chi_i^{O_3}) g_{st,l}^{O_3}. \tag{3}$$

where the leaf internal O_3 concentration ($\chi_i^{O_3}$) is assumed to be zero (Laisk et al., 1989).

The accumulation of ozone fluxes above a threshold of Y $nmol\,m^{-2}(leaf\,area)\,s^{-1}$ ($f_{st,l,Y}$, $nmol\,m^{-2}(leaf\,area)\,s^{-1}$) with

$$f_{st,l,Y} = MAX(0, f_{st,l} - Y) \tag{4}$$

gives the $CUOY_l$. The canopy value of $CUOY$ is calculated by summing $CUOY_l$ over all canopy layers (Franz et al., 2017).

For comparison to observations, the Phytotoxic Ozone Dose (POD, $mmol\,m^{-2}$) can be diagnosed by the accumulation of $f_{st,l}$ for the top canopy layer ($l = 1$), in accordance with LRTAP-Convention (2010) and Büker et al. (2015). The accumulation of ozone fluxes of the top canopy layer above a threshold of y $nmol\,m^{-2}(leaf\,area)\,s^{-1}$ gives the $PODy$. The estimates of $PODy$ (both $POD2$ and $POD3$) can be used off-line to re-construct dose-response relationships equivalent to those described in Büker et al. (2015). These modelled dose-response relationships can then be compared with the empirically derived dose-response relationships to assess the ability of the model to estimate injury. As such, the $POD2$ and $POD3$ used for the formation of these modelled dose-response relationships are purely diagnostic variables and not involved in the injury calculation of the model. The flux thresholds (2 and 3 $nmol\,m^{-2}(leaf\,area)\,s^{-1}$) are not the flux thresholds that are used to estimate biomass response in the O-CN model simulations.

Ozone injury, i.e. the fractional loss of carbon uptake associated with ozone uptake $d_l^{O_3}$, is calculated as a linear function of the cumulative leaf-level uptake of ozone above a threshold of Y $nmol\,m^{-2}(leaf\,area)\,s^{-1}$ ($CUOY_l$)

$$d_l^{O_3} = a - b \times CUOY_l \tag{5}$$

where a is the intercept and b is the slope of the injury function. The injury fraction ($d_l^{O_3}$) is calculated separately for each canopy layer l based on the specific accumulated ozone uptake of the respective canopy layer ($CUOY_l$), and takes values between 0 and 1. The magnitude of $d_l^{O_3}$ in Eq. 5 varies between the canopy layers because $CUOY_l$ varies driven by within-canopy gradients in stomatal conductance and photosynthetic capacity.

The effect of ozone injury on plant carbon uptake is calculated by

$$x_l^{O_3} = x_l(1 - d_l^{O_3}). \tag{6}$$

where x_l is either leaf-level net photosynthesis $A_{n,l}$ or the maximum photosynthetic capacity ($J_{max,l}$ and $V_{cmax,l}$), which is used in the calculation of $A_{n,l}$. J$_{max,l}$ and $V_{cmax,l}$ are reduced in proportion such that the ratio between the two is not altered. While there is some evidence that ozone can affect the ratio between J$_{max}$ and V_{cmax}, we believe that for the purpose of this paper it is justifiable to assume a fixed ratio between them.

Reductions in A_n, l cause a decline in stomatal conductance ($g_{st,l}$) due to the tight coupling between both. Other stress factors that impact $g_{st,l}$ are accounted for in the preceding calculation of the $g_{st,l}$ uninjured by ozone (see Eq. 1). Reductions in $g_{st,l}$ decrease the O_3 uptake into the plant ($f_{st,l}$) and slow the increase in $CUOY_l$ and thus ozone injury.

2.2 Model set-up

Four published injury functions were applied within the O-CN model (see Tab. 1 for the respective slopes, intercepts and flux thresholds). As shown below in Fig. 1 and explained in the results section these did not match well with the observed biomass dose-response relationships by Büker et al. (2015). Following this we manually calibrated two additional injury relationships, one each for A_n or V_{cmax}, based on the data presented in Büker et al. (2015) (see Tab. 1 for slopes and intercepts). For these calibrated injury functions, we chose a flux threshold value of 1 $nmol\,m^{-2}(leaf\ area)\,s^{-1}$, as suggested by LRTAP-Convention (2017). We forced the intercept (a) of these relationships to one to simulate zero ozone injury at zero accumulated O_3 (for ozone levels that cause less then 1 $nmol\,m^{-2}(leaf\ area)\,s^{-1}$ instantaneous ozone uptake). As described above, in all model versions, ozone injury is calculated independently for each canopy layer based on the accumulated O_3 uptake ($CUOY_l$) in that layer, above a specific flux threshold of Y $nmol\,m^{-2}(leaf\ area)\,s^{-1}$ for the respective injury function (see Tab. 1).

Table 1. Slopes and intercepts, partly PFT specific, of all four published (W07$_{PS}$, L12$_{PS}$, L12$_{VC}$, L13$_{PS}$) and two tuned (tun$_{PS}$, tun$_{VC}$) injury functions included in O-CN. Targets of ozone injury are net photosynthesis (PS) or V_{cmax}. Injury calculations base on the $CUOY$ with a specific flux threshold for each injury function.

ID	Target	Slope (b)	Intercept (a)	Plant group	Flux threshold $[nmol\,m^{-2}(leaf\ area)\,s^{-1}]$	Reference
W07$_{PS}$	PS	0.0022	0.9384	All	0	Wittig et al. (2007)
L12$_{PS}$	PS	0.2399	1.0421	All	0.8	Lombardozzi et al. (2012a)
L12$_{VC}$	V_{cmax}	0.1976	0.9888	All	0.8	Lombardozzi et al. (2012a)
L13$_{PS}$	PS	0	0.8752	Broadleaf	0.8	Lombardozzi et al. (2013)
L13$_{PS}$	PS	0	0.839	Needleleaf	0.8	Lombardozzi et al. (2013)
tun$_{PS}$	PS	0.065	1	Broadleaf	1	tuned here
tun$_{PS}$	PS	0.021	1	Needleleaf	1	tuned here
tun$_{VC}$	V_{cmax}	0.075	1	Broadleaf	1	tuned here
tun$_{VC}$	V_{cmax}	0.025	1	Needleleaf	1	tuned here

2.3 Model and protocol for young trees

Single point simulations were run for each fumigation experiment using meteorological input from the daily CRU-NCEP climate data set (CRU-NCEP version 5; LSCE (http://dods.extra.cea.fr/store/p529viov/cruncep/V5_1901_2013/) at the nearest grid cell to the coordinates of the experiment sites. The meteorological data provided by the experiments were incompletely describing the atmospheric boundary conditions required to drive the O-CN model. Atmospheric CO_2 concentrations were taken from Sitch et al. (2015), and reduced as well as oxidised nitrogen deposition in wet and dry forms were provided by the EMEP model (Simpson et al., 2014). Hourly O_3 concentrations were obtained from the experiments, as in Büker et al. (2015).

Büker et al. (2015) report data for eight tree species at 11 sites across Europe (see Tab. A.2 for experiment and simulation details). The O-CN model simulates twelve plant functional types (PFT's) rather than explicit species, therefore the species from the experiments were assigned to the corresponding PFT: All broadleaved species except *Quercus ilex* were assigned to the temperate broadleaved summergreen PFT. *Quercus ilex* was classified as temperate broadleaved evergreen PFT. All needle-leaved species were assigned to the temperate needle-leaved evergreen PFT.

The field experiments were conducted on young trees or cuttings. Prior to the simulation of the experiment, the model was run in an initialisation phase from bare ground until the simulated stand-scale tree age was stable and representative of 1-2 year old seedlings. During this initialisation, O-CN was run with the climate of the years preceding the experiment and zero atmospheric O_3 concentrations. Using ambient ozone concentrations during the initialisation phase would have resulted in different initial biomass values for the different response functions, which would have reduced the comparability of the different model runs. The impact of the ozone concentrations in the initialisation phase on our results here can be considered negligible since we only evaluate the simulated biomass from different treatments in relation to each other and do not evaluate it in absolute terms.

The duration of the initialisation phase depends on the site and PFT and averages 7.8 years (mean over all simulated experiments). Some of the published injury functions and/or parameterisations applied have intercepts unequal to one (a in Eq. 5; see Tab. 1), which induces reductions ($a < 1$) or increases ($a > 1$) in photosynthesis at zero ozone concentration and thus causes a bias in biomass and in particular foliage area at the end of the initialisation phase. To eliminate this bias, the nitrogen-specific photosynthetic capacity of a leaf was adjusted for each of the six parameterisations of the model to obtain comparable LAI values at the beginning of the experiment (see Tab. A.1). This adaption of the nitrogen-specific photosynthetic capacity of a leaf only counterbalances the fixed increases or decreases in the calculation of photosynthesis implied by the intercepts unequal to 1 and has no further impact on ozone uptake and injury calculations.

The simulations of the experiments relied on the meteorological and atmospheric forcing of the experiment years. Simulations were made for all reported O_3 treatments of the specific experiment, including the respective control treatments. Büker et al. (2015) obtained estimates of biomass reductions due to ozone by calculating the hypothetical biomass at zero ozone uptake for all experiments that reported ozone concentrations greater than zero for the control group (e.g. for charcoal filtered or non-filtered air) and calculated the biomass damage from the treatments against a completely undamaged biomass. Our model allows us to run simulations with zero ozone concentrations and skip the calculation of the hypothetical biomass at zero ozone

concentrations as done by Büker et al. (2015). Following this, we ran additional reference simulations with zero O_3 and based our biomass damage calculations upon them.

2.4 Modelling protocol for mature trees

To test whether biomass dose-response relationships of mature forests will show a similar relationship as observed in the simulations of young trees, we ran additional simulations with mature trees. To allow the development of a mature forest where biomass accumulation reached a maximum, and high, and medium turnover soil pools reached an equilibrium, the model was run for 300 years in the initialisation phase. The simulations were conducted with the respective climate previous to the experiment period and zero atmospheric O_3 concentration. For the simulation years previous to 1901 the yearly climate is randomly chosen from the years 1901-1930. Constant values of atmospheric CO_2 concentrations are used in simulated years previous to 1750 followed by increasing concentrations up to the experiment years. The subsequent experiment years are simulated in the same way as the simulations with the young trees. The ozone injury for mature trees is calculated based on the same tun_{VC} injury function (see Tab. 1) that is used in the simulation of young trees.

2.5 Calculation of the biomass damage relationships

The ozone induced biomass damage is calculated from the difference between a treatment and a control simulation. At each experiment site and for all treatments the annual reduction in biomass due to ozone (RB) is calculated as in Büker et al. (2015):

$$RB = \left(\frac{BM_{treat}}{BM_{zero}} \right)^{\frac{1}{n}}, \tag{7}$$

where BM_{treat} represents the biomass of a simulation, which experienced an O_3 treatment and BM_{zero} the biomass of the control simulation with zero atmospheric O_3 concentration. The exponent imposes an equal fractional biomass reduction across all simulation years for experiments lasting longer than one year.

Büker et al. (2015) report the dose-response relationships for biomass reduction with reference to the Phytotoxic Ozone Dose ($PODy$) with flux thresholds y of 2 and 3 $nmol\,m^{-2}(leaf\ area)\,s^{-1}$ (POD_2 and POD_3) for the needleleaf and broadleaf category, respectively, where the $PODy$ values were derived from simulations with the DO_3SE model (Emberson et al., 2000) given site-specific meteorology and ozone concentrations. To be able to compare the simulated biomass reduction by O-CN with these estimates, we also diagnosed these $PODy$ values for each simulation from the accumulated ozone uptake of the top canopy layer ($PODy_{O-CN} = CUOY_{l=1}$). Note that the $PODy_{O-CN}$ is purely diagnostic, and not used in the injury calculations, which are based on the $CUOY_l$ (see Eq. 5). As O-CN computes continuous, half-hourly values of ozone uptake (see Franz et al. (2017) for details), the $PODy_{O-CN}$ values have to be transformed to be comparable to the simulated mean annual $PODy$ values reported in Büker et al. (2015). For deciduous species, the yearly maximum of $PODy_{O-CN}$ was taken as yearly increment $PODy_{O-CN,i}$. The $PODy_{O-CN}$ of evergreen species was continuously accumulated over several

years. To obtain the yearly increment $PODy_{O-CN,i}$, the $PODy_{O-CN}$ at the beginning of the year i is subtracted from the $PODy_{O-CN}$ at the end of the year i.

The selected yearly $PODy_{O-CN,i}$ were used to calculate mean annual values necessary for the formation of the dose-response relationships integrating all simulation years ($PODy^{dr}$) as

$$PODy_i^{dr} = \frac{\sum_{k=1}^{i} PODy_{O-CN,i}}{i} \tag{8}$$

where $PODy_{O-CN,i}$ is the $PODy$ of the i-th year calculated by O-CN. The $PODy^{dr}$ values are used to derive biomass dose-response relationships.

Separate biomass dose-response relationships were estimated by grouping site data for broadleaved and needleleaved species. The biomass dose-response relationships are obtained from the simulation output by fitting a linear model to the simulated values of RB and $PODy^{dr}$ (with flux thresholds of 2 and 3 $nmol\,m^{-2}(leaf\,area)\,s^{-1}$ for needleleaved and broadleaved species, respectively), where the regression line is forced through one at zero $PODy^{dr}$. Büker et al. (2015) report two alternative dose-response relationships for their data set, the simple and the standard model, B_SI and B_ST, respectively. We evaluate our different model versions regarding their ability to reach, with the biomass-dose-response relationships computed from their output, the area between those two functions (target area). The tuned injury relationships tun$_{PS}$ and tun$_{VC}$ were obtained by adjusting the slope b in Eq. 5 such that the corresponding biomass dose-response relationships fits the target area. The intercept of the injury relationships are forced to 1 to simulate zero ozone injury at ozone fluxes lower than 1 $nmol\,m^{-2}(leaf\,area)\,s^{-1}$.

3 Results

3.1 Testing published injury functions

None of the versions where ozone injury is calculated based on previously published injury functions fit the observations well. Some versions strongly overestimate the simulated biomass dose-response relationship and others strongly underestimate it (see Fig. 1) compared to the dose-response relationships developed by Büker et al. (2015).

In the W07$_{PS}$ simulations, where injury is calculated based on the injury function by Wittig et al. (2007), biomass damage is strongly underestimated compared to the estimates from Büker et al. (2015). Ozone injury estimates are mainly driven by the intercept of the relationship, which assumes a reduction of net photosynthesis by 6.16% at zero ozone uptake. Little additional ozone damage occurs due to the accumulation of ozone uptake. As a consequence, the ozone treatments and reference simulations differ little in their simulated biomass. Similarly, the Lombardozzi et al. (2013) injury function (L13$_{PS}$) calculates ozone injury as a fixed reduction of net photosynthesis independent of the actual accumulated ozone uptake. The reference simulations with zero atmospheric ozone thus equals the simulations with ozone treatments and results in an identical simulated biomass. We tested accounting for effects of ozone on stomatal conductance besides net photosynthesis as suggested by Lombardozzi et al. (2013). However, this additional direct injury to stomatal conductance yielded a minimal decrease in simulated biomass accumulation in needle-leaved trees, but did not qualitatively change the results (results not shown). These

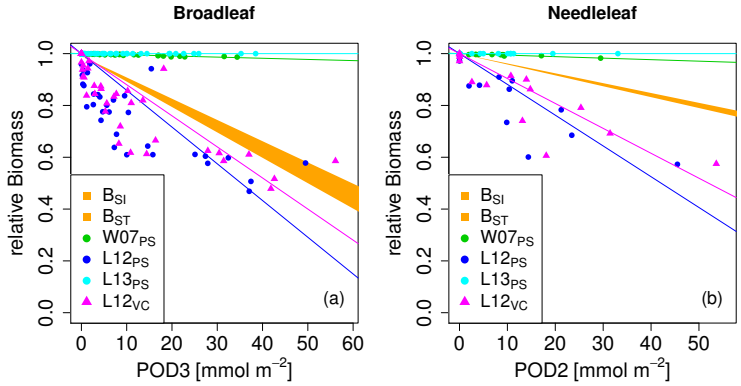

Figure 1. Biomass dose-response relationships for simulations based on published injury relationships, separate for a) broadleaved species, and b) needle-leaved species. The dose-response relationships by Büker et al. (2015), B_{SI} and B_{ST}, define the target area (orange). The displayed dose-response relationships are simulated by model versions which base injury calculations either on net photosynthesis W07$_{PS}$ (Wittig et al., 2007), L12$_{PS}$(Lombardozzi et al., 2012a), and L13$_{PS}$ (Lombardozzi et al., 2013), or on V_{cmax} L12$_{VC}$ (Lombardozzi et al., 2012a) (see Tab. 1 for more details). See Tab. A.3 and A.4 for slopes, intercepts, R^2 and p-values of the displayed regression lines. Injury calculation in the simulations bases on $CUOY$ (see Tab. 1) and not on $POD2$ or $POD3$ (see Sec. 2.5 for more details).

results indicate that injury functions, with a large intercept and a very shallow (or non-existing) slope cannot simulate the impact of spatially varying O_3 concentrations or altered atmospheric O_3 concentrations.

The simulations L12$_{PS}$ and L12$_{VC}$ (net photosynthesis and V_{cmax} injury according to Lombardozzi et al. (2012a), respectively) strongly overestimate biomass damage compared to Büker et al. (2015). Both injury functions assume an extensive injury to carbon fixation at low ozone accumulation values ($CUOY$) of about 5 $mmol\ O_3$. This results in a very steep decline in relative biomass at low values of $POD3$. Notably, despite a linear injury function, the very steep initial decline in biomass of broadleaved trees at low values of $POD3$ is not continued at higher exposure, resulting in a non-linear biomass dose-response relationships. Higher accumulation of ozone doses does not result in higher injury rates beyond a threshold of about 5 $mmol\ O_3\ m^{-2}$ leaf area, and relative biomass declines remain 50 to 70 %. Whereas non-linear dose-response relationships are observed in experiments e.g. for leaf injury (Marzuoli et al., 2009), such a non-linear relationship is not produced in the biomass dose-response relationship by Büker et al. (2015).

We investigated the cause for this at the example of the *Pinus halepensis* stand in the Ebro Delta with a high ozone treatment as shown in Fig. 2. The simulated $CUOY$ quickly increases after the onset of fumigation (Fig. 2a) and is paralleled by a rapid decline in canopy integrated net photosynthesis (A_n^{can}, see Fig. 2b). Once all canopy layers accumulated more than 5 $mmol\ O_3\ m^{-2}$, the canopy photosynthesis is fully reduced, and A_n^{can} becomes negative as a consequence of ongoing leaf maintenance respiration. Thereafter, leaf and total biomass steadily decline (Fig. 2c,d), and the plants are kept alive only by the consumption of stored non-structural carbon reserves. Despite the 100 % reduction in gross photosynthesis, the biomass compared to a control simulation (relative biomass, RB) reaches only values of approximately 0.7 (Fig. 2e), because of the remaining woody and root tissues (see Eq. 7 for the calculation of RB).

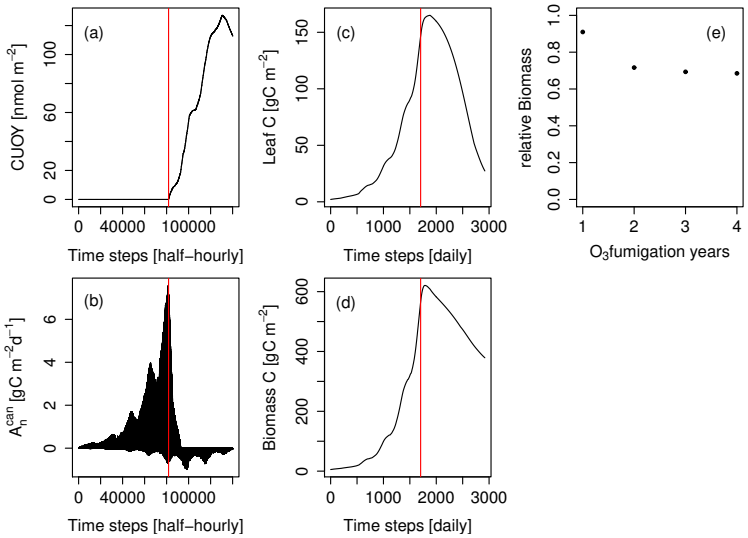

Figure 2. Simulated cumulative ozone uptake above a threshold of 0.8 $nmol\,m^{-2}(leaf\ area)\,s^{-1}$ ($CUOY$), canopy integrated net photosynthesis (A_n^{can}), leaf carbon content ($Leaf\ C$), total carbon in biomass ($Biomass\ C$) and relative Biomass (RB) of *Pinus halepensis* at the Ebro Delta fumigated with the NF+ ozone treatment. Simulations are conducted with the L12$_{PS}$ model version. Panels a-d display the entire simulation period. The red line indicates the onset of O_3 fumigation (NF+) in the 5th of 8 simulations years. The relative biomass compared to a control simulation with zero O_3 concentration (panel e) is displayed for the O_3 fumigation years.

3.2 Tuned injury relationships

We next tested whether a linear injury function is in principle able to reproduce the observed biomass dose-response relationships. Simulations conducted with our tuned injury relationships produce biomass dose-response relationships which fit the target area defined by the B_{SI} and B_{ST} dose-response relationships by Büker et al. (2015) (see Fig. 3 and Tab. A.5, A.6). For the calibrated relationships used in these simulations, we chose a flux threshold value of 1 $nmol\,m^{-2}(leaf\ area)\,s^{-1}$, as suggested by LRTAP-Convention (2017). We forced the intercept (a) of these relationships through 1, to simulate zero ozone injury at ozone fluxes lower than 1 $nmol\,m^{-2}(leaf\ area)\,s^{-1}$. The resulting slope of the tun$_{PS}$ function for broadleaved PFTs is approximately 30 times higher compared to the slope suggested by Wittig et al. (2007) and a fourth of the slope by Lombardozzi et al. (2012a). For the needle-leaved PFT, the tuned slope (tun$_{PS}$) is approximately 10 times higher (lower) than the slopes by Wittig et al. (2007) and Lombardozzi et al. (2012a), respectively. Notably, we did not observe any difference in the model performance irrespective of whether net photosynthesis or photosynthetic capacity (V_{cmax} and simultaneously J_{max}) was reduced.

3.3 Ozone injury to mature trees

The simulation of young trees (simulated as in the previous section) compared to adult trees with the same model version reveals a distinct difference between the simulated versus observed dose-response relationship when expressed as reduction of biomass. Ozone injury causes a much shallower simulated biomass dose-response relationship for adult trees (tun$_{VC}^{mature}$ in

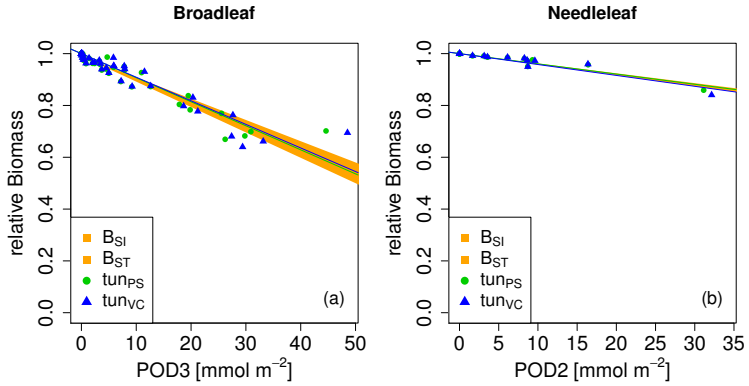

Figure 3. Biomass dose-response relationships for simulations based on tuned injury functions (see Tab. 1 for abbreviations), separate for a) broadleaved species, and b) needle-leaved species. The dose-response relationships by Büker et al. (2015), B_{SI} and B_{ST}, define the target area (orange). See Tab. A.5 and A.6 for slopes, intercepts, R^2 and p-values of the displayed regression lines. Injury calculation in the simulations base on $CUO1$ (see Tab. 1) and not on $POD2$ or $POD3$ (see Sec. 2.5 for more details).

Fig. 4a,b) compared to young trees (tun_{VC}^{young} in Fig. 4a,b), both for broadleaved and needle-leaved species. It is worth noting that this is primarily the consequence of the higher initial biomass of the adult trees before ozone fumigation starts (tun_{VC}^{mature}). Comparing the dose-response relationship of young and mature trees based on the annual net biomass production (NPP) shows nearly identical slopes for needle-leaved species (Fig. 4d and Tab. 3), whereas the slopes for broadleaved tree species (Fig. 4c and Tab. 2) suggests only a slightly lower reduction in NPP in mature compared to young trees, likely related to the larger amount of non-structural reserves that increases the resilience of mature versus young trees.

Table 2. Slopes and intercepts of biomass (RB) and NPP (RN) dose-response relationships (DRR) for broadleaved species simulated by the tun_{VC} model version (see Tab. 1). The fumigation of young trees (tun_{VC}^{young}) with O_3 is compared to the fumigation of mature trees (tun_{VC}^{mature}).

DRR	ID	Intercept (a)	Slope (b)	R^2	p-value
RB	tun_{VC}^{young}	1	0.0091	0.93	5e-25
RB	tun_{VC}^{mature}	1	0.00142	0.91	9.8e-23
RN	tun_{VC}^{young}	1	0.0167	0.96	6.2e-30
RN	tun_{VC}^{mature}	1	0.0144	0.93	1.4e-24

Table 3. Slopes and intercepts of biomass (RB) and NPP (RN) dose-response relationships (DRR) for needle-leaved species simulated by the tun$_{VC}$ model version (see Tab. 1). The fumigation of young trees (tun$_{VC}^{young}$) with O_3 is compared to the fumigation of mature trees (tun$_{VC}^{mature}$).

DRR	ID	Intercept (a)	Slope (b)	R^2	p-value
RB	tun$_{VC}^{young}$	1	0.0042	0.93	2.2e-09
RB	tun$_{VC}^{mature}$	1	0.000785	0.79	4.2e-06
RN	tun$_{VC}^{young}$	1	0.00858	0.97	2.3e-12
RN	tun$_{VC}^{mature}$	1	0.00808	0.99	3 .7e-16

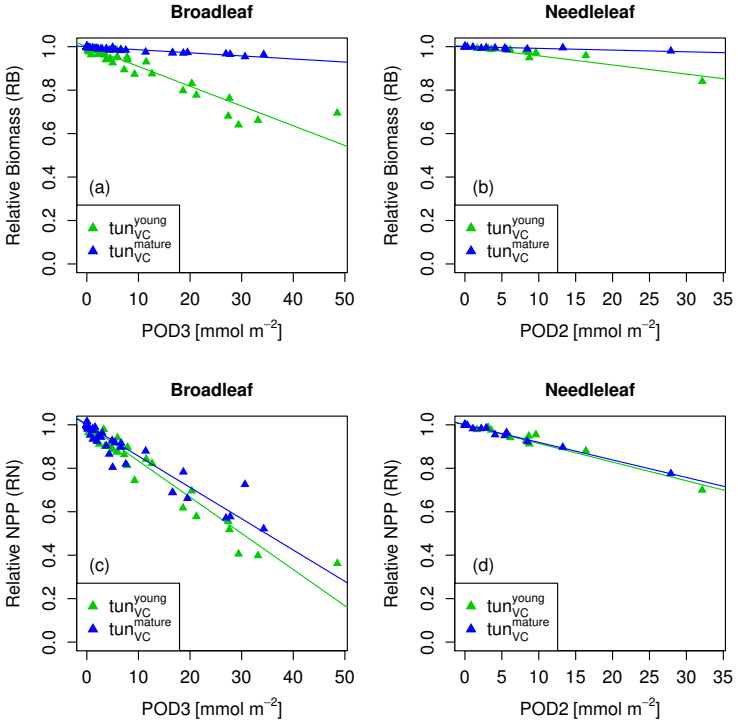

Figure 4. Biomass (RB) and NPP (RN) dose-response relationships of simulations with young (tun$_{VC}^{young}$) and mature trees (tun$_{VC}^{mature}$) separate for a,c) Broadleaf species, and b,d) Needleleaf species.

4 Discussion

Injury functions that relate accumulated ozone uptake to fundamental plant processes such as photosynthesis are a key component for models that aim to estimate the potential impacts of ozone pollution on forest productivity, growth and carbon

sequestration. We tested four published injury functions for net photosynthesis and V_{cmax} within the framework of the O-CN model to assess their ability to reproduce the empirical whole tree biomass dose-response relationships derived by Büker et al. (2015). The biomass dose-response relationships calculated from the O-CN simulations show that the parameterisation of the injury functions included in the model have a large impact on the simulated whole tree biomass: the published injury functions either substantially over- or substantially under-estimated whole tree biomass reduction compared to the data presented by Büker et al. (2015).

The simulation results from the O-CN version applying a injury function based on a single, ozone-sensitive species (Lombardozzi et al., 2012a) to a range of European tree species leads to a strong overestimation of the simulated biomass damage compared to the observations used in this study. The problem of using such injury parameterisations based on short-term experiments of ozone-sensitive species is further highlighted when applying them in simulations of multiple season fumigation experiments and/or high ozone concentrations. Under such conditions, fumigation with high O_3 concentrations can lead to lethal doses, which might not be observed in field experiments due to restricted experiment lengths. Previous studies have suggested that in large areas of Europe, the Eastern US and South-East Asia average growing season values of $CUOY$ for recent years range between 10-100 $mmol\ O_3\ m^{-2}$ (Lombardozzi et al., 2015; Franz et al., 2017). The injury relationships $L12_{PS}$ and $L12_{VC}$ by Lombardozzi et al. (2012a) assume a 100% injury to net photosynthesis or V_{cmax} at accumulation values of about 5 $mmol\ O_3\ m^{-2}$. This would imply that in these large geographic regions, photosynthesis would have been completely impaired by ozone, which is clearly not the case. This result highlights the need for a representative set of species for the development of injury functions for large-scale biosphere models. Overall, our results suggests that the estimates of global GPP reduction as a result of ozone pollution by Lombardozzi et al. (2012a) are strongly overestimated.

Meta-analyses (Wittig et al., 2007; Lombardozzi et al., 2013) are designed to minimise the effect of species-specific ozone sensitivities and provide estimates of the average species response. However, we found that the relationships derived by these meta-analyses substantially underestimate biomass damage. Technically, the reasons for this are a weak or non-existent increase of the ozone injury with increased ozone uptake (shallow or non-existent slopes) and/or high ozone injury at zero accumulated ozone uptake (intercept lower than one). Apparently, the diversity of species responses and experimental settings that are assembled in the meta-analyses by Wittig et al. (2007) and Lombardozzi et al. (2013), together with uncertainties in precisely estimating accumulated ozone uptake in these databases preclude the identification of injury functions that are consistent with the damage estimates by Büker et al. (2015). The high intercepts in the meta-analyses by Wittig et al. (2007) and Lombardozzi et al. (2013), which assume a considerable injury fraction even when no ozone is taken up at all, seem to be ecologically illogical and suggest that an alternative approach is necessary to simulate ozone injury. As a consequence of these points, the Europe-wide GPP reduction estimates by Franz et al. (2017), which has been based on the injury function by Wittig et al. (2007), may substantially underestimate actual GPP reduction. Similarly, global estimates as well as spatial variability of ozone damage to GPP by Lombardozzi et al. (2015), based on Lombardozzi et al. (2013), are virtually independent of actual ozone concentrations or uptake for all tree plant functional types and should be interpreted with caution.

A crucial aspect in forming dose-response relationships is the calculation of the accumulated ozone uptake (e.g. $PODy$ or $CUOY$). The calculation of accumulated ozone uptake is realised in different ways in the meta-analyses and the study by Büker

et al. (2015) as well as in our approach here. Experiments synthesised in the meta-analyses generally do not have access to stomatal conductance values at high resolution measured throughout the experiment, which impedes precise determination of O_3 uptake. The uncertainty in the necessary approximations of accumulated ozone uptake can be assumed to be considerable, and it is thus highly recommendable to measure and report required observations in future ozone fumigation experiments. Büker et al. (2015) use the DO_3SE model to simulate ozone uptake and accumulation similar as done in our model here. These modelled values for ozone uptake and accumulation can assumed to be more reliable since both models simulate processes that determine ozone uptake continuously for the entire experiment length at high temporal resolution. They account for diurnal changes in stomatal conductance as well as climate factors restricting stomatal conductance and hence ozone uptake. However, both models vary in their complexity of the simulated plants, carbon assimilation, and growth processes, which will also impact the estimates of ozone accumulation ($PODy$) and hence their suggested biomass dose-response-relationships.

The meta-analyses do not account for non-stomatal ozone deposition (e.g. to the leaf cuticle or soil), which imposes a bias towards overestimating ozone uptake and accumulation contrary to the DO_3SE model used by Büker et al. (2015), which accounts for this. The O-CN model in principle can simulate non-stomatal ozone deposition from the free atmosphere to ground level (see Franz et al. (2017)). The leaf boundary layer is implicitly included into the calculation of the aerodynamic resistance of O-CN and included in Franz et al. (2017). However, for the simulation of the chamber experiments we used the observed chamber O_3 concentrations, rather than estimating the canopy-level O_3 concentration based on the free atmosphere (approximately 45 m above the surface) and atmospheric turbulence. This required not accounting for aerodynamic resistance and therefore the leaf-boundary layer resistance as well as it prevented the calculation of the non-stomatal deposition, which may lead to a slight overestimation of ozone uptake and accumulation in our simulations.

The calibration of injury functions to net photosynthesis and V_{cmax} shows that in principle, the linear structure of Eq. 5 is sufficient to simulate biomass dose-response relationships comparable to Büker et al. (2015) in O-CN. An advantage of the injury functions derived here compared to previously published injury functions (Wittig et al., 2007; Lombardozzi et al., 2012a, 2013) is the intercept of one, implying that simulated ozone injury is zero at zero accumulated O_3 and steadily increases with increased ozone accumulation. The flux threshold used in the simulations is 1 $nmol\,m^{-2}(leaf\,area)\,s^{-1}$ as suggested by the LRTAP-Convention (2017). Since the tuned injury functions are structurally identical to previously published injury functions based on accumulated ozone uptake they can be directly compared to them. Slopes of the tuned injury functions lie in between the values proposed by Wittig et al. (2007) and Lombardozzi et al. (2012a) and thus take values in an expected range. We did not find any significant difference in simulated biomass responses between the use of net photosynthesis or leaf-specific photosynthetic capacity (V_{cmax}) as a target for the ozone injury function, although we do note that the slopes were slightly lower for the net photosynthesis based functions. The simulation of ozone effects on leaf-specific photosynthetic capacity (V_{cmax}) seems preferable over the adjustment of net photosynthesis, because V_{cmax} and J_{max} are parameters in the calculation of net photosynthesis, and thus are likely easier transferable between models. Models with different approaches to simulate net photosynthesis might obtain better comparable results by using injury relationships that target V_{cmax} instead of net photosynthesis.

All injury functions included into the O-CN model base injury calculations on the injury index $CUOY$ (canopy value) rather than $PODy$, as used by some other models, e.g. the DO_3SE model (Emberson et al., 2000). We tested the effect of basing the injury calculation on $POD1$ rather than $CUO1$, and found that these produced comparable biomass dose-response relationships as the injury relationships based on $CUO1$ presented in Fig. 3 (results not shown). The slopes of injury functions based on $POD1$ are approximately two thirds and half compared to the slopes based on $CUO1$ for broadleaved and needle-leaved species, respectively. The difference in the slope values associated with $POD1$ and $CUO1$ results from the different calculation, and application of them. $PODy$ is calculated in the top canopy layer and the respective injury fraction is then applied uniformly to all canopy layers. $CUOY$ and the associated injury fraction is calculated separately for each canopy layer and varies with the canopy profile of stomatal conductance, and therefore the distribution of light and photosynthetic capacity (other factors such as vertical gradients of temperature or ozone are currently not represented in OCN). More analysis of the gradients of ozone injury within deep canopies are required to evaluate whether the scaling of top-of-the-canopy injury to whole canopy injury is appropriate or if alternative simulation approaches need to be developed. Higher frequency data on the ozone injury incurred by plants are required to disentangle whether an ozone injury parameterisation based on instantaneous (e.g. similar to the approach by Sitch et al. (2007)) or accumulated ozone uptake results in a more accurate simulation of the seasonal effects of ozone fumigation.

Further aspects that determine ozone sensitivity and damage to carbon gain of plants like leaf morphology (Calatayud et al., 2011; Bussotti, 2008), different sensitivity of sunlit and shaded leafs (Tjoelker et al., 1995; Wieser et al., 2002), early senescence (Gielen et al., 2007; Ainsworth et al., 2012) and costs for detoxification of ozone and/or repair of ozone injury that likely increases the plant's respiration costs (Dizengremel, 2001; Wieser and Matyssek, 2007) are not considered by either approach. Marzuoli et al. (2016) observed an ozone induced reduction of biomass but no significant reduction in physiological parameters like V_{cmax}. They suggest that the reduced growth is caused by higher energy investments and reducing power for the detoxification of ozone whereas the photosynthetic apparatus remained uninjured (Marzuoli et al., 2016).

Species within the same plant functional type are known to exhibit different sensitivities to ozone (Wittig et al., 2007, 2009; Mills et al., 2011; Büker et al., 2015). This suggests that the application of a single injury function for a large set of species and plant functional types may not be sufficient to yield reliable estimates of large scale damage estimates. Species interaction and competition, differing genotypes and individuals ontogeny may further alter ozone impacts on plants and ecosystems (Matyssek et al., 2010). For instance, a modelling study using an individual-based forest model showed that ozone may not reduce the carbon sequestration capacity in forests if at the ecosystem level the reduced carbon fixation of ozone-sensitive species are compensated for by an increased carbon fixation of less ozone-sensitive species (Wang et al., 2016). First generation dynamic global vegetation models such as OCN do not simulate separate species but are based on plant functional types, which combine a large set of species. This restricts *per se* the ability of global models to simulate ozone-induced community dynamics, and may therefore lead to overestimates of the net ozone impact if the parameterisation of the damage functions is entirely based on ozone-sensitive species. In our study, we have presented an approach to use the existing experimental evidence to parameterise a globally applicable model in a simple design to generate injury functions which are based on a relevant range of species

rather than relying on species-specific injury functions as a first step towards a more reliable parameterisation of large-scale ozone damage.

Some studies have found that ozone-affected stomata respond much slower to environmental stimuli than unaffected cells (Paoletti and Grulke, 2005), which can delay closure and trigger, stomatal sluggishness, an uncoupling of stomatal conductance and photosynthesis (Reich, 1987; Tjoelker et al., 1995; Lombardozzi et al., 2012b) and thus impact transpiration rates (Mills et al., 2009; Paoletti and Grulke, 2010; Lombardozzi et al., 2012b) and the plant's water use efficiency (Wittig et al., 2007; Mills et al., 2009; Lombardozzi et al., 2012b). The O-CN model is able to directly impair stomatal conductance, by uncoupling injury to net photosynthesis from the subsequent injury to stomatal conductance. In this version of the O-CN model both net photosynthesis and stomatal conductance can directly be injured by individual injury functions. The simulation of this kind of direct injury to stomatal conductance additional to the injury of net photosynthesis, both according to the injury functions by (Lombardozzi et al., 2013), have a negligible impact on biomass production compared to not accounting for direct injury to the stomata (results not shown). However, our above mentioned concerns regarding the structure of the injury relationships by Lombardozzi et al. (2013) should be taken into account when considering this result.

A key challenge for the use of fumigation experiments to parameterise ozone-injury in models is that trees (as opposed to grasses fumigated from seeds) typically possess a certain amount of biomass at the beginning of the fumigation experiment. Even at lethal ozone doses, the relative biomass thus can not decline to zero, and tree death may occur at values of a relative biomass greater than zero. The relative biomass is positive even if carbon fixation is fully reduced and the plants survive due to the use of stored carbon. The higher the initial biomass and the slower the annual biomass growth rate of the tree is, the harder it is to obtain low values of RB. When comparing RB values obtained from trees with substantial different initial biomass and tree species with different growth rates proportionate damage rates thus can not directly be inferred. This indicates that the explanatory value of the relative biomass between a control and a treatment to estimate long-term plant damage at a given O_3 concentration is limited. This is particularly the case when evaluating the damage of more mature forests. The simulated biomass dose-response relationships of adult trees are much more shallow than dose-response relationships of young trees (see Fig. 4), because of the high initial biomass prior to fumigation. This suggests that the use of biomass injury functions derived from experiments with young trees to parameterise the biomass loss of adult trees, as done in Sitch et al. (2007), will likely lead to an overestimation of plant damage and loss of carbon storage. Dose-response relationships based on biomass increments or growth rates might be better transferable between saplings and mature trees and hence better suitable to be used for parameterising global terrestrial biosphere models.

Our approach to overcome this challenge was to alter the vegetation model to simulate the ozone damage of small trees, where we could directly compare simulated biomass reductions to observations. Since we used injury relationships that are based on the calculation of leaf-level photosynthesis, we are able to apply the calibrated model also for mature stands. Our simulations have demonstrated that despite the different sizes of young and mature trees, and associated changes in the wood growth rate and the available amount of non-structural carbon reserves to repair incurred injury, the simulated effect of ozone on the net annual biomass production (NPP) was very similar, when using a injury function associated with leaf-level photosynthesis. Overall our findings support the idea that the photosynthesis-based injury relationships developed here and evaluated

against fumigation experiments of young trees, might be useful to estimate effect on forest production of older trees. Monitoring approaches of ozone damage that are either capable of measuring the actual increment of biomass, or quantify at the leaf and canopy level the change in net photosynthesis over the growing season, would allow to develop injury/damage estimates that could be more readily translated into modelling frameworks.

The extrapolation of results from short-term experiments with young trees to estimate responses of adult trees grown under natural conditions is subject to several issues, e.g. due to the differing environmental conditions and changing ozone sensitivities with increasing tree size or age (Schaub et al., 2005; Cailleret et al., 2018). If the simulation of injury to photosynthesis based on experiments with young trees can indeed be transferred to adult trees to yield realistic biomass damage estimates is still uncertain. The sparse knowledge of ozone effects on the biomass of adult forest trees prevents an evaluation of simulated ozone damage of adult trees. Ozone fumigation is mostly found to reduce e.g. biomass or diameter of adult trees (e.g. Matyssek et al. (2010) for an overview), but this is not always the case (Samuelson et al., 1996; Percy et al., 2007). Results from phytotron and free-air fumigation studies suggest that in natural forests a multitude of abiotic and biotic factors exist that have the potential to impact the plants ozone effects (Matyssek et al., 2010). If more data become available e.g. of the changes in ozone sensitivity between young and mature trees a more realistic damage parameterisation of mature forests in terrestrial biosphere models might become possible.

Terrestrial biosphere models in general assume that plant growth is primarily determined by carbon uptake. However, an alternative concept proposes that plant growth is more limited by direct environmental controls (temperature, water and nutrient availability) than by carbon uptake and photosynthesis (Fatichi et al., 2014). The O-CN model provides a first step into this direction because it separates the step of carbon acquisition from biomass production, both in terms of a non-structural carbon buffer, as well as a stoichiometric nutrient limitation on growth independent of the current photosynthetic rate. This would in principle allow to account for ozone effects on the carbon sink dynamics within plants. However, it is not clear that data readily exist to parameterise such effects. Instead of targeting net photosynthesis as done in our approach here, ozone injury might be better simulated by targeting biomass growth rates or processes that limit these e.g. stomatal conductance, which impacts the plants water balance, given that suitable data to parameterise a large scale model become available.

All in all, a multitude of aspects that impact ozone damage to plants is not yet incorporated into global terrestrial biosphere models. The ongoing discussion which processes are major drivers for observed damage, how they interact and impact different species and plant types plus the lack of suitable data needed to parameterise a global model are reasons why the simulation of ozone damage up to now focuses only on a few aspects where suitable data are available as presented in our study.

5 Conclusion

The inclusion of previously published injury functions into the terrestrial biosphere model O-CN led to a strong over- or underestimation of simulated biomass damage compared to the biomass dose-response relationship by Büker et al. (2015). Injury functions included into terrestrial biosphere models are a key aspect in the simulation of ozone damage and have a great impact on the estimated damage. The calibration of injury functions performed in this study provide the advantage to

calculate ozone injury close to where the actual physiological injury might occur (photosynthetic apparatus) and simultaneously reproduce observed biomass damage relationships for a range of European forest species used by Büker et al. (2015). The calibration of ozone injury functions similar to our approach here in other ozone sub-models of terrestrial biosphere models might improve damage estimates compared to previously published injury functions and might lead to better estimates of terrestrial carbon sequestration. The comparison of simulated biomass dose-response relationships of young and mature trees shows strongly different slopes. This suggests that observed biomass damage relationships from young trees might not be suitable to estimate biomass damage of mature trees. The comparison of simulated NPP dose-response relationships of young and mature trees show similar relationships and suggests that they might more readily be transferred between trees differing in age.

Acknowledgements. We would like to thank Per Erik Karlsson of the IVL Swedish Environmental Research Institute, Göteborg, Sweden, Sabine Braun of the Institute for Applied Plant Biology, Witterswil, Switzerland, and Gerhard Wieser of the Federal Research and Training Centre for Forests, Natural Hazards and Landscape (BFW), Innsbruck, Austria for providing collected data from their ozone fumigation experiments. This research leading to this publication was supported by the EU Framework programme through grant no. 282910 (ECLAIRE), and the Max Planck Society for the Advancement of Science e.V. through the ENIGMA project. This project has received funding from the European Research Council (ERC) under the European Union's Horizon 2020 research and innovation programme (grant agreement no. 647204; QUINCY).

Table A.1. Original and adapted values of the nitrogen specific photosynthetic capacity of a leaf (npl) for three out of four different O-CN versions (ID) including published injury functions. The intercept of the fourth O-CN version ($L12_{VC}$) is very close to one and simulations produce comparable LAI values without an adaption of npl.

ID	PFT	npl original	npl adapted
$W07_{PS}$	Broadleaf	1.50	1.60
$W07_{PS}$	Needleleaf	0.75	0.80
$L12_{PS}$	Broadleaf	1.50	1.45
$L12_{PS}$	Needleleaf	0.75	0.70
$L13_{PS}$	Broadleaf	1.50	1.75
$L13_{PS}$	Needleleaf	0.75	0.90

Table A.2. List of fumigation experiments used by Büker et al. (2015) and simulated here.

Site	Longitude [°E]	Latitude [°N]	Species	O_3 treatment start year	Fumigation [yrs]
Östad (S)	12.4	57.9	*Betula pendula*	1997	2
Birmensdorf (CH)	8.45	47.36	*Betula pendula*	1989	1
Birmensdorf (CH)	8.45	47.36	*Betula pendula*	1990	1
Birmensdorf (CH)	8.45	47.36	*Betula pendula*	1992	1
Birmensdorf (CH)	8.45	47.36	*Betula pendula*	1993	1
Kuopio (FIN)	27.58	62.21	*Betula pendula*	1994	2
Kuopio (FIN)	27.58	62.21	*Betula pendula*	1996	3
Kuopio (FIN)	27.58	62.21	*Betula pendula*	1994	5
Schönenbuch (CH)	7.5	47.54	*Fagus sylvatica*	1991	2
Zugerberg (CH)	8.54	47.15	*Fagus sylvatica*	1987	2
Zugerberg (CH)	8.54	47.15	*Fagus sylvatica*	1989	3
Zugerberg (CH)	8.54	47.15	*Fagus sylvatica*	1991	2
Curno (I)	9.03	46.17	*Populus spec.*	2005	1
Grignon (F)	1.95	48.83	*Populus spec.*	2008	1
Ebro Delta (SP)	0.5	40.75	*Quercus ilex*	1998	3
Col-du-Donon (F)	7.08	48.48	*Quercus robur or petraea*	1999	2
Headley (U.K.)	-0.75	52.13	*Quercus robur or petraea*	1997	2
Ebro Delta (SP)	0.5	40.75	*Pinus halepensis*	1993	4
Col-du-Donon (F)	7.08	48.48	*Pinus halepensis*	1997	2
Schönenbuch (CH)	7.5	47.54	*Picea abies*	1991	2
Zugerberg (CH)	8.54	47.15	*Picea abies*	1991	2
Östad (S)	12.4	57.9	*Picea abies*	1992	5
Headley (U.K.)	-0.75	52.13	*Pinus sylvestris*	1995	2

Table A.3. Slopes and intercepts of biomass dose-response relationships for broadleaved species simulated by O-CN versions based on published injury functions to net photosynthesis or V_{cmax} (see Tab. 1). B_{SI} and B_{ST} represent the simple and standard model of Büker et al. (2015).

ID	Intercept (a)	Slope (b)	R^2	p-value
B_{SI}	0.99	0.0082	0.34	<0.001
B_{ST}	0.99	0.0098	0.38	<0.001
$W07_{PS}$	1	0.00045	0.93	1e-24
$L12_{PS}$	1	0.0142	0.77	2e-14
$L15_{PS}$	1	0.0000	NaN	NaN
$L12_{VC}$	1	0.0120	0.80	1.9e-15

Table A.4. Slopes and intercepts of biomass dose-response relationships for needle-leaved species simulated by O-CN versions based on published injury functions to net photosynthesis or V_{cmax} (see Tab. 1). B_{SI} and B_{ST} represent the simple and standard model by Büker et al. (2015).

ID	Intercept (a)	Slope (b)	R^2	p-value
B_{SI}	1	0.0038	0.46	<0.001
B_{ST}	1	0.0042	0.52	<0.001
$W07_{PS}$	1	0.00058	0.93	1.5e-09
$L12_{PS}$	1	0.0119	0.83	9.4e-07
$L15_{PS}$	1	0.0000	NaN	NaN
$L12_{VC}$	1	0.0096	0.85	3.5e-07

Table A.5. Slopes and intercepts of biomass dose-response relationships for broadleaved species simulated by O-CN versions based on tuned injury functions to net photosynthesis or V_{cmax} (see Tab. 1). B_{SI} and B_{ST} represent the simple and standard model by Büker et al. (2015).

ID	Intercept (a)	Slope (b)	R^2	p-value
B_{SI}	0.99	0.0082	0.34	<0.001
B_{ST}	0.99	0.0098	0.38	<0.001
tun_{PS}	1	0.0093	0.94	1.4e-26
tun_{VC}	1	0.0091	0.93	5e-25

Table A.6. Slopes and intercepts of biomass dose-response relationships for needle-leaved species simulated by O-CN versions based on tuned injury functions to net photosynthesis or V_{cmax} (see Tab. 1). B_{SI} and B_{ST} represent the simple and standard model by Büker et al. (2015).

ID	Intercept (a)	Slope (b)	R^2	p-value
B_{SI}	1	0.0038	0.46	<0.001
B_{ST}	1	0.0042	0.52	<0.001
tun_{PS}	1	0.0039	0.94	4.8e-10
tun_{VC}	1	0.0042	0.93	2.2e-09

References

Ainsworth, E. A., Yendrek, C. R., Sitch, S., Collins, W. J., and Emberson, L. D.: The Effects of Tropospheric Ozone on Net Primary Productivity and Implications for Climate Change*, Annual review of plant biology, 63, 637–661, 2012.

Ball, J., IE, W., and JA, B.: A model predicting stomatal conductance and its contribution to the control of photosynthesis under different environmental conditions, Prog. Photosynthesis Res. Proc. Int. Congress 7th, Providence. 10-15 Aug 1986, pp 221–224, 1987.

Büker, P., Feng, Z., Uddling, J., Briolat, A., Alonso, R., Braun, S., Elvira, S., Gerosa, G., Karlsson, P., Le Thiec, D., Marzuoli, R., Mills, G., Oksanen, E., Wieser, G., , Wilkinson, M., and Emberson, L.: New flux based dose-response relationships for ozone for European forest tree species, Environmental Pollution, 206, 163–174, https://doi.org/10.1016/j.envpol.2015.06.033, http://tinyurl.sfx.mpg.de/ug3q, 2015.

Bussotti, F.: Functional leaf traits, plant communities and acclimation processes in relation to oxidative stress in trees: a critical overview, Global Change Biology, 14, 2727–2739, 2008.

Cailleret, M., Ferretti, M., Gessler, A., Rigling, A., and Schaub, M.: Ozone effects on European forest growth—Towards an integrative approach, Journal of Ecology, 106, 1377–1389, 2018.

Calatayud, V., Cerveró, J., Calvo, E., García-Breijo, F.-J., Reig-Armiñana, J., and Sanz, M. J.: Responses of evergreen and deciduous Quercus species to enhanced ozone levels, Environmental Pollution, 159, 55–63, 2011.

Dizengremel, P.: Effects of ozone on the carbon metabolism of forest trees, Plant Physiology and Biochemistry, 39, 729–742, 2001.

Emberson, L., Simpson, D., Tuovinen, J., Ashmore, M., and Cambridge, H.: Towards a model of ozone deposition and stomatal uptake over Europe, EMEP MSC-W Note, 6, 1–57, 2000.

Fatichi, S., Leuzinger, S., and Koerner, C.: Moving beyond photosynthesis: from carbon source to sink-driven vegetation modeling, NEW PHYTOLOGIST, 201, 1086–1095, https://doi.org/10.1111/nph.12614, 2014.

Feng, Z. and Kobayashi, K.: Assessing the impacts of current and future concentrations of surface ozone on crop yield with meta-analysis, Atmospheric Environment, 43, 1510–1519, 2009.

Franz, M., Simpson, D., Arneth, A., and Zaehle, S.: Development and evaluation of an ozone deposition scheme for coupling to a terrestrial biosphere model, Biogeosciences, 14, 45–71, https://doi.org/10.5194/bg-14-45-2017, http://www.biogeosciences.net/14/45/2017/, 2017.

Friend, A.: Modelling canopy CO2 fluxes: are 'big-leaf'simplifications justified?, Global Ecology and Biogeography, 10, 603–619, 2001.

Gielen, B., Löw, M., Deckmyn, G., Metzger, U., Franck, F., Heerdt, C., Matyssek, R., Valcke, R., and Ceulemans, R.: Chronic ozone exposure affects leaf senescence of adult beech trees: a chlorophyll fluorescence approach., Journal of experimental botany, 58, 785–795, https://doi.org/10.1093/jxb/erl222, http://tinyurl.sfx.mpg.de/ueyt, 2007.

Guderian, R.: Air Pollution. Phytotoxicity of Acidic Gases and Its Significance in Air Pollution Control, Springer-Verlag, New York., 1977.

Hanson, P., Samuelson, L., Wullschleger, S., Tabberer, T., and Edwards, G.: Seasonal patterns of light-saturated photosynthesis and leaf conductance for mature and seedling Quercus rubra L. foliage: differential sensitivity to ozone exposure, Tree Physiology, 14, 1351–1366, 1994.

Harmens, H. and Mills, G.: Ozone Pollution: Impacts on carbon sequestration in Europe, NERC/Centre for Ecology & Hydrology, 2012.

Karlsson, P. E., Uddling, J., Braun, S., Broadmeadow, M., Elvira, S., Gimeno, B., Le Thiec, D., Oksanen, E., Vandermeiren, K., Wilkinson, M., et al.: New critical levels for ozone effects on young trees based on AOT40 and simulated cumulative leaf uptake of ozone, Atmospheric Environment, 38, 2283–2294, 2004.

Kolb, T. and Matyssek, R.: Limitations and perspectives about scaling ozone impacts in trees, Environmental Pollution, 115, 373–393, 2001.

Krinner, G., Viovy, N., de Noblet-Ducoudré, N., Ogée, J., Polcher, J., Friedlingstein, P., Ciais, P., Sitch, S., and Prentice, I.: A dynamic global vegetation model for studies of the coupled atmosphere-biosphere system, Global Biogeochem. Cycles, 19, GB1015, https://doi.org/10.1029/2003GB002199, 2005.

Laisk, A., Kull, O., and Moldau, H.: Ozone concentration in leaf intercellular air spaces is close to zero, Plant Physiology, 90, 1163–1167, 1989.

Li, P., Feng, Z., Catalayud, V., Yuan, X., Xu, Y., and Paoletti, E.: A meta-analysis on growth, physiological and biochemical responses of woody species to ground-level ozone highlights the role of plant functional types, Plant, Cell & Environment, 2017.

Lombardozzi, D., Levis, S., Bonan, G., and Sparks, J.: Predicting photosynthesis and transpiration responses to ozone: decoupling modeled photosynthesis and stomatal conductance, Biogeosciences Discuss, 9, 4245–4283, 2012a.

Lombardozzi, D., Sparks, J., Bonan, G., and Levis, S.: Ozone exposure causes a decoupling of conductance and photosynthesis: implications for the Ball-Berry stomatal conductance model, Oecologia, pp. 1–9, 2012b.

Lombardozzi, D., Sparks, J. P., and Bonan, G.: Integrating O_3 influences on terrestrial processes: photosynthetic and stomatal response data available for regional and global modeling, Biogeosciences Discussions, 10, 6973–7012, https://doi.org/10.5194/bgd-10-6973-2013, http://www.biogeosciences-discuss.net/10/6973/2013/, 2013.

Lombardozzi, D., Levis, S., Bonan, G., Hess, P., and Sparks, J.: The Influence of Chronic Ozone Exposure on Global Carbon and Water Cycles, Journal of Climate, 28, 292–305, 2015.

LRTAP-Convention: Manual on Methodologies and Criteria for Modelling and Mapping Critical Loads and Levels; and Air Pollution Effects, Risks and Trends, http://www.rivm.nl/en/themasites/icpmm/index.html, http://www.rivm.nl/en/themasites/icpmm/index.html, 2010.

LRTAP-Convention: Manual on Methodologies and Criteria for Modelling and Mapping Critical Loads and Levels; and Air Pollution Effects, Risks and Trends, https://icpvegetation.ceh.ac.uk/, https://icpvegetation.ceh.ac.uk/publications/documents/FinalnewChapter3v4Oct2017_000.pdf, 2017.

Marzuoli, R., Gerosa, G., Desotgiu, R., Bussotti, F., and Denti, A. B.: Ozone fluxes and foliar injury development in the ozone-sensitive poplar clone Oxford (Populus maximowiczii x Populus berolinensis): a dose-response analysis., Tree physiology, 29, 67–76, https://doi.org/10.1093/treephys/tpn012, http://tinyurl.sfx.mpg.de/uav6, 2009.

Marzuoli, R., Monga, R., Finco, A., and Gerosa, G.: Biomass and physiological responses of Quercus robur (L.) young trees during 2 years of treatments with different levels of ozone and nitrogen wet deposition, Trees, 30, 1995–2010, 2016.

Massman, W.: A review of the molecular diffusivities of H2O, CO2, CH4, CO, O-3, SO2, NH3, N2O, NO, AND NO2 in air, O-2 AND N-2 near STP, Atmospheric environment, 32, 1111–1127, https://doi.org/10.1016/S1352-2310(97)00391-9, http://tinyurl.sfx.mpg.de/ucen, 1998.

Matyssek, R., Karnosky, D. F., Wieser, G., Percy, K., Oksanen, E., Grams, T. E. E., Kubiske, M., Hanke, D., and Pretzsch, H.: Advances in understanding ozone impact on forest trees: Messages from novel phytotron and free-air fumigation studies, ENVIRONMENTAL POLLUTION, 158, 1990–2006, https://doi.org/10.1016/j.envpol.2009.11.033, 2010.

Mills, G., Hayes, F., Wilkinson, S., and Davies, W.: Chronic exposure to increasing background ozone impairs stomatal functioning in grassland species, Global Change Biology, 15, 1522–1533, 2009.

Mills, G., Pleijel, H., Braun, S., Büker, P., Bermejo, V., Calvo, E., Danielsson, H., Emberson, L., Fernández, I., Grünhage, L., Harmens, H., Hayes, F., Karlsson, P., and Simpson, D.: New stomatal flux-based critical levels for ozone effects on vegetation, Atmospheric Environment, 45, 5064–5068, 2011.

Morgan, P., Ainsworth, E., and Long, S.: How does elevated ozone impact soybean? A meta-analysis of photosynthesis, growth and yield, Plant, Cell & Environment, 26, 1317–1328, 2003.

Niinemets, Ü., Keenan, T. F., and Hallik, L.: A worldwide analysis of within-canopy variations in leaf structural, chemical and physiological traits across plant functional types, New Phytologist, 205, 973–993, 2015.

Nunn, A., Weiser, G., Reiter, I., Häberle, K., Grote, R., Havranek, W., and Matyssek, R.: Testing the unifying theory of ozone sensitivity with mature trees of Fagus sylvatica and Picea abies, Tree physiology, 26, 1391–1403, 2006.

Oliver, R. J., Mercado, L. M., Sitch, S., Simpson, D., Medlyn, B. E., Lin, Y.-S., and Folberth, G. A.: Large but decreasing effect of ozone on the European carbon sink, Biogeosciences Discussions, 2017, 1–32, https://doi.org/10.5194/bg-2017-409, https://www.biogeosciences-discuss.net/bg-2017-409/, 2017.

Paoletti, E. and Grulke, N.: Does living in elevated CO< sub> 2</sub> ameliorate tree response to ozone? A review on stomatal responses, Environmental Pollution, 137, 483–493, 2005.

Paoletti, E. and Grulke, N.: Ozone exposure and stomatal sluggishness in different plant physiognomic classes, Environmental Pollution, 158, 2664–2671, 2010.

Paoletti, E., Contran, N., Bernasconi, P., Günthardt-Goerg, M. S., and Vollenweider, P.: Erratum to" Structural and physiological responses to ozone in Manna ash (Fraxinus ornus L.) leaves of seedlings and mature trees under controlled and ambient conditions", Science of the Total Environment, 408, 2014–2024, 2010.

Percy, K., Nosal, M., Heilman, W., Dann, T., Sober, J., Legge, A., and Karnosky, D.: New exposure-based metric approach for evaluating O3 risk to North American aspen forests, Environmental Pollution, 147, 554–566, 2007.

Pleijel, H., Danielsson, H., Ojanperä, K., Temmerman, L. D., Högy, P., Badiani, M., and Karlsson, P.: Relationships between ozone exposure and yield loss in European wheat and potato—a comparison of concentration-and flux-based exposure indices, Atmospheric Environment, 38, 2259–2269, 2004.

Reich, P.: Quantifying plant response to ozone: a unifying theory, Tree Physiology, 3, 63–91, 1987.

Samuelson, L. and Kelly, J.: Carbon partitioning and allocation in northern red oak seedlings and mature trees in response to ozone, Tree Physiology, 16, 853–858, 1996.

Samuelson, L., Kelly, J., Mays, P., and Edwards, G.: Growth and nutrition of Quercus rubra L. seedlings and mature trees after three seasons of ozone exposure, Environmental Pollution, 91, 317–323, 1996.

Schaub, M., Skelly, J., Zhang, J., Ferdinand, J., Savage, J., Stevenson, R., Davis, D., and Steiner, K.: Physiological and foliar symptom response in the crowns of Prunus serotina, Fraxinus americana and Acer rubrum canopy trees to ambient ozone under forest conditions, Environmental Pollution, 133, 553–567, 2005.

Simpson, D., Christensen, J., Engardt, M., Geels, C., Nyiri, A., Soares, J., Sofiev, M., Wind, P., , and Langner, J.: Impacts of climate and emission changes on nitrogen deposition in Europe: a multi-model study, Atmos. Chem. Physics, 14, 6995–7017, https://doi.org/10.5194/acp-14-0073-2014, http://www.atmos-chem-phys.net/14/0073/2014/acp-14-0073-2014.html, 2014.

Sitch, S., Cox, P., Collins, W., and Huntingford, C.: Indirect radiative forcing of climate change through ozone effects on the land-carbon sink, Nature, 448, 791–794, 2007.

Sitch, S., Friedlingstein, P., Gruber, N., Jones, S. D., Murray-Tortarolo, G., Ahlström, A., Doney, S. C., Graven, H., Heinze, C., Huntingford, C., Levis, S., Levy, P. E., Lomas, M., Poulter, B., Viovy, N., Zaehle, S., Zeng, N., Arneth, A., Bonan, G., Bopp, L., Canadell, J. G., Chevallier, F., Ciais, P., Ellis, R., Gloor, M., Peylin, P., Piao, S. L., Le Quéré, C., Smith, B., Zhu, Z., and Myneni, R.: Recent trends

and drivers of regional sources and sinks of carbon dioxide, Biogeosciences, 12, 653–679, https://doi.org/10.5194/bg-12-653-2015, http://www.biogeosciences.net/12/653/2015/, 2015.

Tjoelker, M., Volin, J., Oleksyn, J., and Reich, P.: Interaction of ozone pollution and light effects on photosynthesis in a forest canopy experiment, Plant, Cell & Environment, 18, 895–905, 1995.

Wang, B., Shugart, H. H., Shuman, J. K., and Lerdau, M. T.: Forests and ozone: productivity, carbon storage, and feedbacks, Scientific reports, 6, 22 133, 2016.

Wieser, G. and Matyssek, R.: Linking ozone uptake and defense towards a mechanistic risk assessment for forest trees, New Phytologist, 174, 7–9, 2007.

Wieser, G., Hecke, K., Tausz, M., Haberle, K., Grams, T., and Matyssek, R.: The role of antioxidative defense in determining ozone sensitivity of Norway spruce (Picea abies (L.) Karst.) across tree age: Implications for the sun-and shade-crown, PHYTON-HORN-, 42, 245–254, 2002.

Wittig, V., Ainsworth, E., and Long, S.: To what extent do current and projected increases in surface ozone affect photosynthesis and stomatal conductance of trees? A meta-analytic review of the last 3 decades of experiments, Plant, cell & environment, 30, 1150–1162, 2007.

Wittig, V., Ainsworth, E., Naidu, S., Karnosky, D., and Long, S.: Quantifying the impact of current and future tropospheric ozone on tree biomass, growth, physiology and biochemistry: a quantitative meta-analysis, Global Change Biology, 15, 396–424, 2009.

Zaehle, S. and Friend, A.: Carbon and nitrogen cycle dynamics in the O-CN land surface model: 1. Model description, site-scale evaluation, and sensitivity to parameter estimates, Global Biogeochemical Cycles, 24, GB1005, http://dx.doi.org/10.1029/2009GB003521, 2010.